A ROBUST H_2 STATE FEEDBACK CONTROLLER APPLIED TO BOOST CONVERTERS

Vinícius F. Montagner◊ Luiz A. Maccari Jr.◊ Humberto Pinheiro◊ Ricardo C. L. F. Oliveira*

◊ Power Electronics and Control Research Group
Federal University of Santa Maria
97105-900, Santa Maria – RS, Brazil

*School of Electrical and Computer Engineering
University of Campinas - UNICAMP
13083-852, Campinas – SP, Brazil

E-mails: vfmontagner@gmail.com luizmaccari@gmail.com humberto.ctlab.ufsm.br@gmail.com ricfow@dt.fee.unicamp.br

***Abstract* - This paper proposes the design and the experimental validation of a robust H_2 control technique applied to boost converters. Differently from conventional techniques, the proposed controller has a certificate of stability and performance under arbitrary parameter variations. The design procedure adopts a linearized model with a polytopic structure for the converter affected by time-varying parameters. An optimal H_2 state feedback controller (under quadratic stability) is synthesized using convex optimization based on linear matrix inequalities. This framework allows the determination of the control gains in a very fast way, using a finite set of inequalities to obtain a controller that ensures robust stability and performance for the entire set of uncertain parameters. An experimental setup of a boost converter is used to validate the controller designed here. The input voltage, the operating point duty cycle and the load are considered as arbitrarily time-varying uncertain parameters. The synthesized control gains produce good simulated and experimental results when compared to those obtained with a classical strategy based on PI controllers, without introducing additional implementation cost. The experimental validation proves the viability of practical application of this important robust control technique for boost converters.**

***Keywords* - Boost Converter, Polytopic Uncertainty, Robust Control, Optimal Control, Linear Matrix Inequalities.**

I. INTRODUCTION

Boost converters are an important class of DC-DC converters used in several applications as hybrid electric vehicles, power factor correction devices, renewable energy conversion systems, etc. The control of boost converters usually aims on regulation of the output voltage, with small under/overshoots and short settling times when recovering from load and input transient, good frequency response and rejection of disturbances [1]. Such performance specifications can be achieved, for instance, by means of state feedback control laws, which are suitable for optimal control and robust control strategies [2-4].

The linear quadratic regulator (LQR) is recognized as one of the most important optimal control techniques, providing good stability margins for the closed-loop system and the reduction of the control signal energy [3]. Such controllers have been used in several applications including power converters [5-8]. The application of a discrete LQR with a state observer for a Cuk converter is presented in [6]. In [9], the authors apply a discrete LQR and a Kalman filter used as a state observer for an AC power source system with linear and nonlinear loads. This technique was also used in [8], for uninterruptible power supply application. These papers deal with the design of discrete-time LQRs, implemented in digital platforms. In the recent work [5], polytopic models for DC-DC converters are used to deal with uncertainty of the duty cycle operating point and of the load parameters. The design of the LQR is formulated in terms of the vertices of a polytopic model using linear matrix inequality (LMI) based conditions [10], providing a controller that is robust against uncertainties. This allows, for instance, the operation of boost converters with large load ranges. Additionally, the resulting controller is suitable for analog implementation, whose advantages and drawbacks are well known [11]. On the other hand, one of the most important difficulties with the design of LQRs is the choice of the weighting matrices, even for robust LQRs. In [7], the problem of finding the weighting matrices for an LQR applied to a boost converter is efficiently solved with the help of a genetic algorithm.

One limitation of using linear control techniques, as the conventional LQR, for a nonlinear plant, as the boost converter, is that the performance of linear controllers designed for a linearized model of the converter may become poor for large perturbation, as for instance load variations in wide ranges [12]. Nonlinear control techniques provide an interesting possibility of controlling the converter for a large range of operation [7, 13]. The difficulty with this approach relies on the fact that nonlinear control techniques are in general complex to be determined. Fuzzy logic based controllers can provide a useful alternative [14], allowing to design local controllers by means of, for instance, linear control techniques, and then combining these controllers with

Artigo submetido em 15/12/2010. Aceito para publicação em 16/02/2011 por recomendação do Editor João Onofre P. Pinto.

fuzzy logic to provide a suitable global controller for nonlinear systems, as given by [7] in the context of the boost converter.

Another alternative to control boost converters presenting a large range of operation is the use of robust control techniques, which can provide controllers that ensure stability and performance for the closed-loop system against uncertain parameters and disturbances [4, 10, 15]. Models including uncertain parameters for power converters have been proposed, for instance, in [16], in the context of linear fractional representation for uncertainty, and in [5] and [17], for polytopic uncertainty. Even though robust control techniques have been investigated in several works available in control literature, their applicability for power converters is an important issue of research. The use of LMIs as a tool for power converters control design can be seen for instance in [17-20], providing efficient mathematical conditions to compute robust and optimal controllers.

The main motivation of this work is that most control techniques applied to boost converters do not take into account parameters with uncertainties, possibly time-varying, when dealing with the design of controllers. Usually, the controller is computed for a nominal model and then, *a posteriori*, the robustness is investigated by means of exhaustive simulation for some chosen points in the set of parameters. This approach cannot guarantee robust stability and performance under parametric variations. Even in the case of uncertain and time-invariant parameters, one has the problem of concluding about closed-loop stability and performance of a set of infinite points testing only some points. This work provides a solution for this problem, leading to a controller with certificate of robust stability which does not rely on exhaustive simulation. In the sequence of the paper, one has the design and experimental validation of a robust H_2 state feedback controller for a boost converter subject to uncertain and time-varying operating point duty cycle, load resistance and input voltage. Up to the knowledge of the authors, this strategy has not been developed, experimentally proven and analyzed for this plant as reported in this paper, being this the main contribution here. A polytopic model is used to represent such uncertainties in a way that the control design condition carried out for a finite number of points is valid for the entire set of uncertainties. Convex optimization with LMI constraints which describe the robust H_2 state feedback control design under quadratic stability is used to compute the control gains. The control design is evaluated for the parameters of a 100 W boost converter prototype and the robust H_2 state feedback control gains are fast determined by means of a commonly used LMI solver [21], leading to optimal performance in terms of rejection of disturbances in the context of H_2 control under quadratic stability. Experimental results demonstrate that the closed-loop system efficiently rejects disturbances from the input voltage and from the load, yielding fast transient responses with no steady-state errors. The cost for implementation of the control law is similar to classical PI based control loops for boost converter. The frequency response indicates a good rejection of disturbances on the input voltage and on the load for the range of frequencies of interest, which corroborates the suitability of the controller for this application.

II. CONVERTER MODELING

Consider the boost converter given in Figure 1

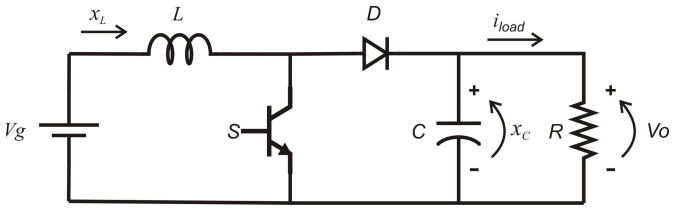

Fig. 1. Boost converter.

where x_L and x_C are the state variables representing, respectively, the inductor current and the capacitor voltage.

A state space averaged model of the converter in continuous conduction mode is given by

$$\begin{aligned}\dot{\tilde{x}}(t) &= (A_{off} + (A_{on} - A_{off})U)\tilde{x}(t) \\ &+ (A_{on} - A_{off})\tilde{x}(t)\tilde{u}(t) \\ &+ ((A_{on} - A_{off})X + (B_{u_{on}} - B_{u_{off}}))\tilde{u}(t)\end{aligned} \quad (1)$$

where A_{on} and $B_{u_{on}}$ are the dynamic and control matrices when the switch is on and A_{off} and B_{off} are the dynamic and control matrices when the switch is off. The incremental and equilibrium input vectors are $\tilde{u}(t)$ and U while the incremental and equilibrium state vectors are $\tilde{x}(t)$ and X, respectively, allowing to write

$$\tilde{u}(t) = \tilde{d}_d(t),\ U = D_d,\ \tilde{x}(t) = \begin{bmatrix}\tilde{x}_L(t) \\ \tilde{x}_C(t)\end{bmatrix}$$

$$X = \begin{bmatrix}X_L^* \\ X_C^*\end{bmatrix} = \begin{bmatrix}\dfrac{V_g}{D'_d{}^2 R} \\ \dfrac{V_g}{D'_d}\end{bmatrix},\ A_{on} = \begin{bmatrix}0 & 0 \\ 0 & -\dfrac{1}{RC}\end{bmatrix}, \quad (2)$$

$$A_{off} = \begin{bmatrix}0 & -\dfrac{1}{L} \\ \dfrac{1}{C} & -\dfrac{1}{RC}\end{bmatrix},\ B_{u_{on}} = B_{u_{off}} = \begin{bmatrix}\dfrac{1}{L} \\ 0\end{bmatrix}$$

where D'_d is the complementary operating point duty cycle given by $D'_d = 1 - D_d$. The conventional linearization and the addition of an extra state variable representing integral action to ensure zero steady state error are taken into account to get the augmented representation of the system (see, for instance, [2] and [18])

$$\begin{aligned}\dot{\tilde{\xi}}(t) &= A\tilde{\xi}(t) + B\tilde{u}(t) \\ \tilde{\xi}(t) &= \begin{bmatrix}\tilde{x}(t) \\ \tilde{\lambda}(t)\end{bmatrix},\ \tilde{\lambda}(t) = -\int_0^t \tilde{x}_C(\tau)\,d\tau\end{aligned} \quad (3)$$

where

$$A=\begin{bmatrix} 0 & -\frac{D'_d}{L} & 0 \\ \frac{D'_d}{C} & -\frac{1}{RC} & 0 \\ 0 & -1 & 0 \end{bmatrix},\quad B=\begin{bmatrix} \frac{V_g}{D'_d L} \\ -\frac{V_g}{{D'_d}^2 RC} \\ 0 \end{bmatrix} \tag{4}$$

Although one knows that the boost converter presents a nonlinear dynamics, this linearized model can be used to design linear state feedback controllers capable to provide robustness for operation under parametric variations, which is the main point to be addressed here. It is plausible to assume that the load parameter *R*, the complementary operating point duty-cycle D'_d and the input voltage *Vg* can be time-varying. When these parameters vary inside given intervals, even when subject to arbitrarily fast variations, one has that (4) can be represented by a polytope of matrices [10, 21]. Including the input vector $w(t)$ to represent disturbances affecting the system and the equation of the system output, $\tilde{y}(t)$, in order to have the conditions for the H_2 control design, the boost converter can be represented by the time-varying polytopic model given by

$$\begin{aligned} \dot{\tilde{\xi}}(t) &= A(\alpha(t))\tilde{\xi}(t)+B(\alpha(t))\tilde{u}(t)+E(\alpha(t))w(t) \\ \tilde{y}(t) &= C(\alpha(t))\tilde{\xi}(t)+D(\alpha(t))\tilde{u}(t) \end{aligned} \tag{5}$$

where

$$\begin{aligned} &A(\alpha(t))=\sum_{i=1}^{N}\alpha_i(t)A_i\,,\ B(\alpha(t))=\sum_{i=1}^{N}\alpha_i(t)B_i\,, \\ &E(\alpha(t))=\sum_{i=1}^{N}\alpha_i(t)E_i\,,\ C(\alpha(t))=\sum_{i=1}^{N}\alpha_i(t)C_i, \\ &D(\alpha(t))=\sum_{i=1}^{N}\alpha_i(t)D_i, \\ &\alpha_i(t)\geq 0, i=1,....,N,\ \sum_{i=1}^{N}\alpha_i(t)=1 \end{aligned} \tag{6}$$

The time dependence of variables $\tilde{\xi}$, $\tilde{u}$, w, $\tilde{y}$ and of the vector of uncertain parameters α is dropped for sake of a simpler notation. The parameter vector α of the polytopic model is supposed as arbitrarily time-varying, thus representing the uncertain parameters of the converter for slow or fast variations, even in the case where the parameters switch from one value to another (instantaneous variations) or when the parameters remain on the same value (time-invariant case) but are not precisely known. Matrices A_i, B_i, C_i, D_i, E_i in (6) are the vertices of the polytope, with appropriate dimensions and real entries, whose values are obtained from the modeling of the problem. This model plays a key role in the design of robust control for the plant. The uncertain parameters are supposed to belong to continuous intervals, leading to a domain with infinite admissible values. Thus, the problem of finding control gains that ensure stability and performance for all the points of the domain is an infinite dimensional problem. In the case the parameters are represented by the polytopic set, one has that a control gain that ensures stability and performance only for the vertices of the polytope (i.e. a finite set) also ensures the same properties for the entire set of uncertainties, thanks to the convexity of the polytopic set [10]. This model allows to apply robust control design as finite dimension problems, with certificate of stability and performance, as follows.

III. ROBUST H_2 STATE FEEDBACK CONTROL

The boost converter shown in Figure 1 is now used with the parameter set presented in Table I in order to design a robust controller and to experimentally validate it.

TABLE I
Parameters of the boost converter

Parameter	Value
Vg	25 V
Vo	50 V
D'_d	0.5
L	886 µH
C	220 µF
f_s	50 kHz

The nominal power of the converter is 100 W. The parameters *R*, D'_d and *Vg* are considered varying arbitrarily inside the intervals

$$R\in[18.75,50]\Omega,\ D'_d\in[0.4,0.6],\ Vg\in[22,48]V \tag{7}$$

Notice that the intervals in (7) are useful to verify robustness of the control for relatively large variations of the parameters and that other different interval for the parameters could be chosen to represent other situations of interest to design a robust controller in the same way presented here. In general, larger intervals tend to lead to more conservative results.

The polytopic model is generated as in [5], including here *Vg* as another independent uncertain parameter to cope with variations on the input voltage.

In order to compute a state feedback control law

$$u=K\tilde{\xi} \tag{8}$$

ensuring robust stability and performance under arbitrary parameter variation, the standard H_2 guaranteed cost control under quadratic stability is used [22].

System (5) is stabilizable by means of the control law (8) if there exists a solution for the convex optimization problem

$$\begin{aligned} &\sigma^* \triangleq \min_{X_d=X_d',Z,W=W'>0} Tr(X_d) \quad s.t. \\ &\begin{bmatrix} X_d & C_iW+D_iZ \\ WC_i'+Z'D_i' & W \end{bmatrix}\geq 0 \\ &\begin{bmatrix} A_iW+WA_i'+B_iZ+Z'B_i' & E_i \\ E_i' & -I \end{bmatrix}\leq 0 \\ &i=1,....,N \end{aligned} \tag{9}$$

In this case,

$$K=ZW^{-1} \tag{10}$$

ensures robust stability in the presence of arbitrary parameter variations with the quadratic Lyapunov function

$$v(\tilde{\xi})=\tilde{\xi}'P\tilde{\xi}\ ,\ P=W^{-1} \tag{11}$$

and performance measured by an H_2 guaranteed cost

$$\rho = \sqrt{\sigma^*} \tag{12}$$

being σ^* the minimum trace of X_d.

This is a well known result in robust control literature and the proof can be found in [22]. Matrices A_i, B_i, C_i, D_i, E_i in (9) are data of the problem and matrices W, Z and X_d are variables to be determined.

Using the system parameters presented in Table I and the intervals given in (7), and choosing the matrices

$$C_i = \begin{bmatrix} \sqrt{Q} \\ 0_{1x3} \end{bmatrix}, \quad D_i = \begin{bmatrix} 0_{3\times1} \\ \sqrt{R_u} \end{bmatrix}, E_i = I_{3\times3} \tag{13}$$

with

$$Q = \begin{bmatrix} 2 & 0 & 0 \\ 0 & 4 & 0 \\ 0 & 0 & 1000000 \end{bmatrix}, \; R_u = 10 \tag{14}$$

one has that the conditions from (9) provide the gains

$$K = \begin{bmatrix} -1.0354 & -0.6874 & 316.1373 \end{bmatrix} \tag{15}$$

and the Lyapunov matrix

$$W = \begin{bmatrix} 125.5915 & -58.3003 & 0.2608 \\ -58.3003 & 363.0972 & 0.6068 \\ 0.2608 & 0.6068 & 0.0022 \end{bmatrix} \tag{16}$$

as the certificate of robust stability for arbitrary parameter variations inside the intervals (7). Using the LMI Control Toolbox from Matlab in a notebook with 1.66 GHz processor and 1 GB of RAM, the gains (15) are calculated in 1.14s. Moreover, from the choice of fixed matrices C_i, D_i and E_i in (13), one has that the problem of robust H_2 control solved here ensures the minimization of the cost function

$$\int_0^\infty (\tilde{\xi}' Q \tilde{\xi} + \tilde{u}' R_u \tilde{u}) dt \tag{17}$$

from the optimal linear quadratic control problem, which can be seen as a special case of the H_2 control problem. The control designer could use other matrices C_i, D_i and E_i, leading to other H_2 guaranteed cost under quadratic stability. Moreover, when the disturbances $w(t)$ are independent zero mean unit variance white noises with power spectral density equal to identity, the RMS value of the output is minimized under quadratic stability. This means optimal rejection of disturbances to the output ensured by the proposed H_2 control approach. The stability ensured by the gains from (15) is asymptotic and robust for system (5). It is also important to mention that other LMI constraints to take into account specifications as, for instance, pole placement in prescribed regions on the left hand side of the complex plane and limitation of the norm of the control signal could be easily added to the optimization problem [10, 21]. However, with the LMIs in (9), one can obtain good results in terms of transient and steady state responses, as given in the next section.

IV. SIMULATION AND EXPERIMENTAL RESULTS

In order to evaluate the designed controller, simulation and experimental tests are carried out. The output of the system is the voltage across the load (*Vo*). The following tests verify the robustness against load and input variations, as well as allow to observe the transient and steady state behavior of the converter with the proposed controller for open-loop and closed-loop operation. A classical controller based on two PIs, one for the current and another for the voltage loop, which is a conventional technique for boost converters, is used for a comparison. In the tests for load variation, the load switches from one resistor of 50 Ω to the parallel association of 30 Ω and 50 Ω and in the tests for input voltage variation, the input *Vg* is varied in the interval (7). The control implementation is analog, using standard operational amplifier circuitry, following the block diagram in Figure 2.

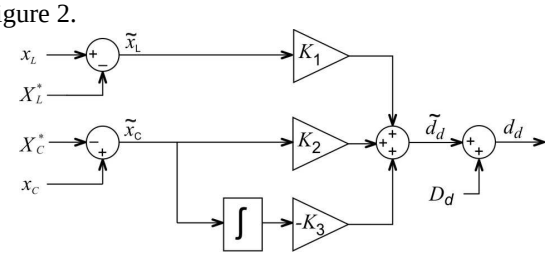

Fig. 2. Block diagram of the control law synthesis.

Figure 3 details the implementation of the PWM signal used to drive switch S in Figure 1, being T the PWM period.

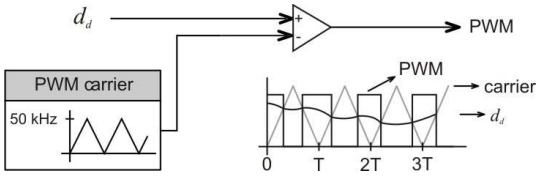

Fig. 3. Block diagram of PWM signal generation.

First, to recall the limitations of the open-loop responses, Figure 4 shows a disturbance on the input voltage and the resulting output voltage. For this test, the duty cycle was set at 0.5. As expected, the disturbance on the input voltage is amplified to the output, leading to a poor performance. Figure 5 shows the results for the sudden variation on the load. One can note slow transients, with oscillations and with large undershoots and overshoots.

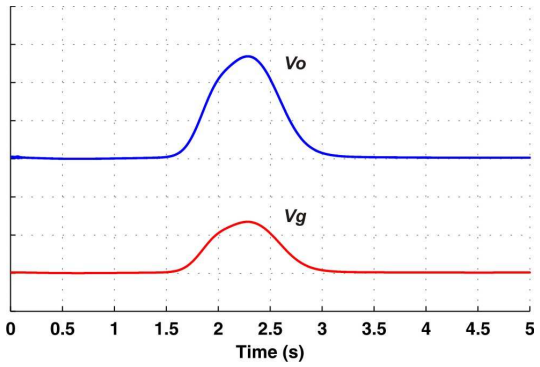

Fig 4. Open-loop simulation result: variation on the input voltage (*Vg* – peak value of 48 V) and resulting output voltage (*Vo* – peak value of 96 V). Scales: *Vg*: 20 V/div and *Vo*: 20 V/div.

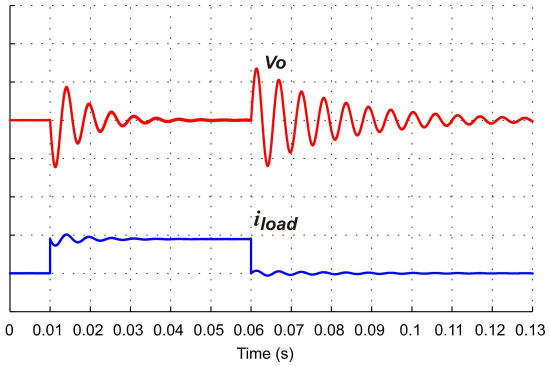

Fig. 5. Open-loop simulation result: variation on the load current (i_{load} with initial value of 1 A) and resulting output voltage (*Vo* with initial value of 50 V). Scales: 2 A/div and 5 V/div.

The closed-loop performance with the robust H_2 control gains (15) is superior. Notice from Figure 6 (in comparison with Figure 4) that the input voltage variation practically does not affect the output voltage, indicating that the closed-loop system provides very good rejection of the input disturbance. The result for the load variation for the system with the robust controller is shown in Figure 7. The most important aspect to mention is that the quality of this response is significantly better than in terms of under/overshoots, settling times and oscillations to the open-loop response in Figure 5.

In order to have a more stringent comparison, the results of a controller based on one PI for the current loop and another for the voltage loop (see, for instance [23-24]), designed for the nominal power condition, with the aim of ensuring phase and gain margins greater than 60° and 20 dB, respectively, are illustrated jointly with the results of the H_2 controller in Figure 8. The conventional strategy leads to a poorer performance, without any prior guarantee of robustness against parametric variations. On the other hand, the robust H_2 control can cope with arbitrary parametric variations, providing good performance.

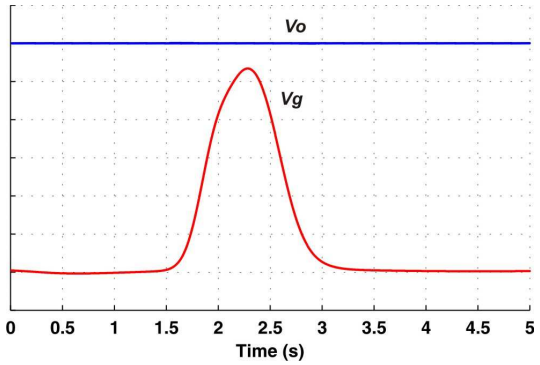

Fig. 6. Closed-loop simulation result: variation on the input voltage (*Vg* – peak value of 48 V) and resulting variation of output voltage (*Vo* = 50 V) with the robust H_2 controller. Scales: *Vg*: 5 V/div and *Vo*: 2 V/div.

Simulations indicate that the robust H_2 controller can ensure good results for the plant. However, the experimental validation is important to prove the viability of the controller since in practice one has problems as actuator saturation and other unmodeled dynamics that can lead to a deteriorated performance.

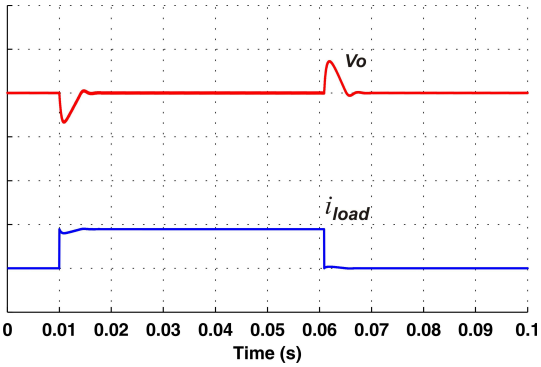

Fig. 7. Closed-loop simulation result: variation on the load current (i_{load} with initial value of 1 A) and resulting output voltage (*Vo* with initial value of 50 V) with the robust H_2 controller. Scales: 2 A/div and 5 V/div.

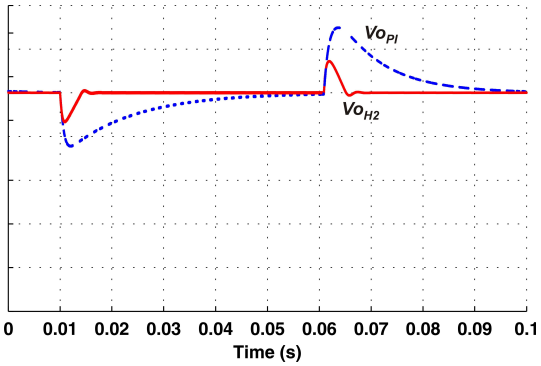

Fig. 8. Closed-loop simulation result: variation on the load current and resulting output voltage (*Vo* with initial value of 50 V) with the robust H_2 controller (Vo_{H2}) and conventional controller based on two PIs (Vo_{PI}). Scale 5 V/div.

Figure 9 shows the experimental results for the same input disturbance test investigated in Figure 6. The good capacity of rejection of the input voltage disturbance is confirmed by means of the experimental results. In addition, a good correspondence between the simulated and the experimental results is obtained.

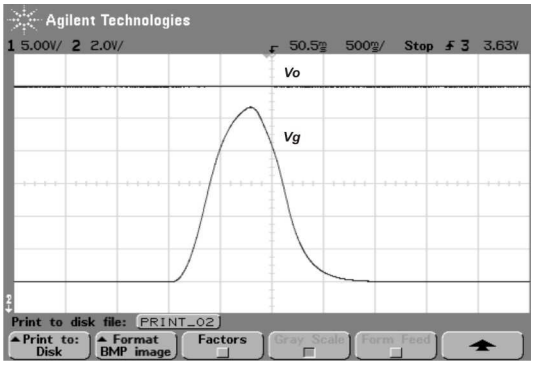

Fig. 9. Closed-loop experimental result: variation on the input voltage (*Vg* – peak value of 48 V) and resulting variation of output voltage (*Vo* = 50 V). Scales:*Vg*: 5 V/div and *Vo*: 2 V/div.

Figure 10 presents the experimental results for the same load variation given by Figure 7. Again, a good

correspondence between simulated and experimental results is observed, indicating that the robust H_2 controller produces good experimental results for rejection of the load disturbance.

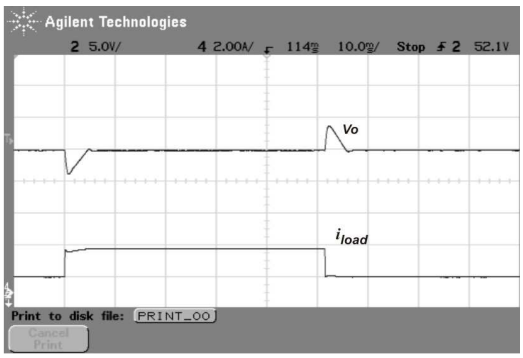

Fig. 10. Closed-loop experimental result: variation on the load current (i_{load} with initial value of 1 A) and resulting output voltage (*Vo* with initial value of 50 V).

Figure 11 and Figure 12 show, respectively, details on the undershoot and overshoot presented in Figure 10. One can see an undershoot of 7.74% and a settling time of 4 ms in Figure 11. An overshoot of 7.84% and a settling time of 3.8 ms can be seen in Figure 12. These waveforms confirm good transient responses for the switching load, representing instantaneous variations on this parameter.

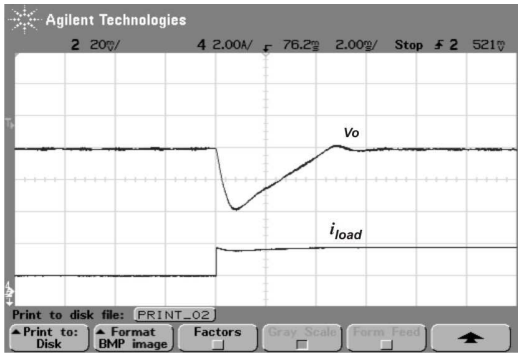

Fig. 11. Closed-loop experimental result: detail of load current increase (i_{load} with initial value of 1 A) and resulting output voltage (*Vo* with initial value of 50 V).

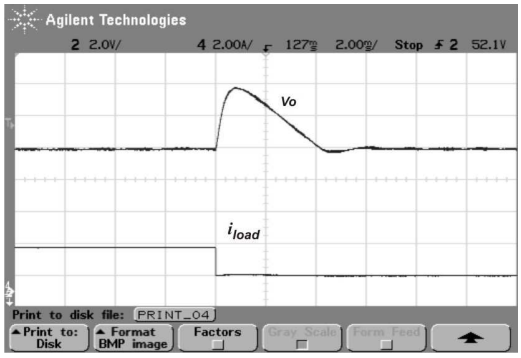

Fig. 12. Closed-loop experimental result: detail of load current decrease (i_{load} with final value of 1 A) and resulting output voltage (*Vo* with final value of 50 V).

In order to have an easier comparison of the simulation and experimental waveforms, the tests from Figure 11 and Figure 12 are reproduced together with the respective simulation results in Figure 13 and Figure 14. The error between both waveforms is small, corroborating the validation of the controller.

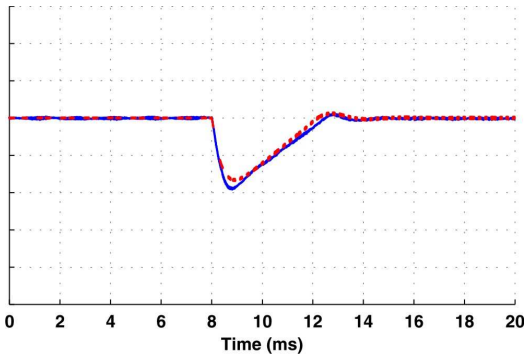

Fig. 13. Comparison of the experimental results (continuous line) from Figure 11 and the respective simulation results (dashed line).

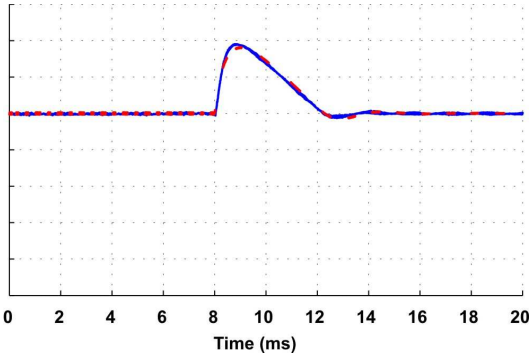

Fig. 14. Comparison of the experimental results (continuous line) from Figure 12 and the respective simulation results (dashed line).

It is worth to mention that the state space controller (8) used here is equivalent to a proportional controller of the current loop (first entry of control vector gain *K*) and a PI controller of the voltage loop (second and third entries of control vector gain *K*) of the boost converter. Thus, its complexity is lower than the classical control based on a PI controller for each loop which is widely used for this converter. The gains provided here are valid for the system with uncertain and time-varying parameters while the gains from the classical design method are only valid for the system supposed as perfectly known and time-invariant. Additionally, another good feature of the proposed strategy is that the time spent for control design in (9) is short when compared to that from the classical control design based on the iterative computation of two PI controllers.

V. REJECTION OF DISTURBANCES

The capacity of rejection of disturbances of the boost converter with the proposed controller is investigated in this section in a small signal analysis framework. Consider the converter with a disturbance on the input voltage and a disturbance on the load current, as illustrated in Figure 15 by the two additional sources, which represent any small signal.

The nominal linearized model in (3) with an additional matrix to represent the disturbance entries is written as

$$\dot{\tilde{\xi}}(t) = A\tilde{\xi}(t) + B\tilde{u}(t) + F\tilde{w}(t) \qquad (18)$$

where

$$F' = \begin{bmatrix} 1/L & 0 & 0 \\ 0 & -1/C & 0 \end{bmatrix}, \ \tilde{w} = \begin{bmatrix} \tilde{v}_g \\ \tilde{i}_o \end{bmatrix}$$

with F given in its transpose form.

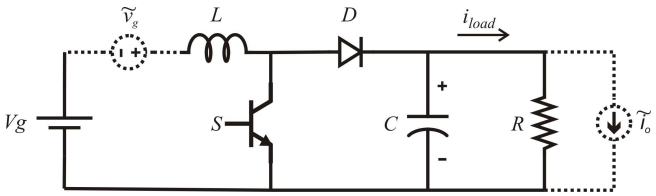

Fig. 15. Boost converter with disturbances on the input voltage and on the load current.

The analysis of rejection of disturbances is evaluated by means of the frequency response in closed-loop with gains given by (15) and considering the voltage across the capacitor as the system output. First, consider only $\tilde{v}_g$ as the input disturbance (i.e. $\tilde{i}_o = 0$). For this situation, one has the magnitude of the Bode diagram given in Figure 16.

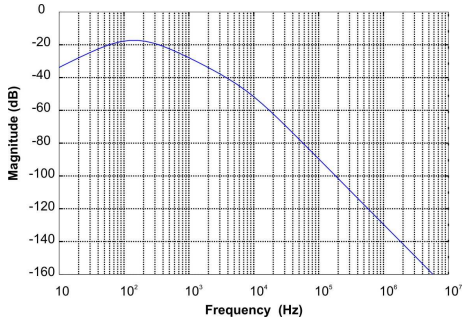

Fig. 16. Magnitude Bode Diagram from disturbances on the input voltage to the output voltage.

It is immediate to observe that the closed-loop system with robust H_2 control has a very good capacity of rejection of variations from the input voltage for the entire range of frequencies. This explains the results in Figure 6.

A more stringent evaluation concerns the rejection of disturbances on the load current $\tilde{i}_o$. The closed-loop system has the frequency response given by Figure 17.

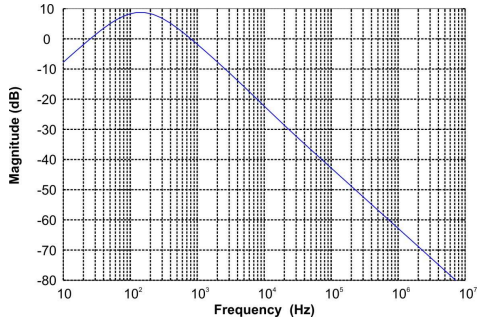

Fig. 17. Magnitude Bode Diagram from disturbances on the load current to the output voltage.

Notice a good capacity of rejection of disturbances, except for one range of frequencies where the closed-loop system produces amplifications. This behavior is corroborated by means of simulations of the closed-loop system for sinusoidal disturbances $\tilde{i}_o$ with the frequencies given in Table II. This table shows the comparison between the steady state gains from the frequency response (Figure 17) and the gains obtained by means of the waveforms from the closed-loop circuit simulation.

TABLE II
Gains from the frequency response

Frequency (Hz)	Gain from Bode Diagram	Gain from circuit simulation
60	2.03	2.09
120	2.72	2.77
143	2.76	2.70
180	2.69	2.66

The results by Figure 16 and Figure 17 allow to determine limits of operation for the closed-loop system. Small disturbances on the input voltage will be well rejected in all frequencies and small disturbances on the load current will have poorer rejection around 120 Hz. Loads with harmonic current with frequencies around this value, as for instance PWM inverters, can be also used with the closed-loop system respecting limits of power to have acceptable variation on the output voltage.

VI. CONCLUSION

This paper presented a robust state feedback controller design for a boost converter subject to load, operating point duty cycle and input voltage variations. The converter is modeled in a polytopic description taking into account parametric uncertainty. The uncertain parameters are arbitrarily time-varying. The control gains, including a state feedback gain for integral action, are obtained from convex optimization conditions for H_2 guaranteed cost control under quadratic stability and thus the closed-loop system is stable for the entire set of uncertainties, under fast parameter variation. This strategy has not been developed, validated in practice and analyzed for this plant as reported here, being this the main contribution. Several tests are performed for the converter subject to variations on the input voltage and on the load. The waveforms prove a good correspondence between simulation and experimental results and demonstrate the robustness and superior performance of the closed-loop system. The frequency response also corroborated the good capacity of rejection of disturbances of the closed-loop system with the robust H_2 controller, whose implementation cost is comparable to that from classical controllers.

ACKNOWLEDGEMENTS

Grants from the Brazilian Agencies CAPES and CNPq.

REFERENCES

[1] R. W. Erickson, *Fundamentals of power electronics*. New York: Chapman & Hall, 1997.

[2] R. C. Dorf and R. H. Bishop, *Modern control systems*, 11 ed. Upper Saddle River, USA: Prentice Hall, 2008.

[3] P. Dorato, C. T. Abdallah, and V. Cerone, *Linear quadratic control: an introduction*. Malabar, USA: Krieger Pub. Co., 2000.
[4] K. Zhou, J. C. Doyle, and K. Glover, *Robust and optimal control*. Upper Saddle River, USA: Prentice Hall, 1996.
[5] C. Olalla, R. Leyva, A. El Aroudi, and I. Queinnec, "Robust LQR Control for PWM Converters: An LMI Approach," *IEEE Transactions on Industrial Electronics*, vol. 56, pp. 2548-2558, Jul 2009.
[6] F. H. F. Leung, P. K. S. Tam, and C. K. Li, "An Improved Lqr-Based Controller for Switching Dc-Dc Converters," *IEEE Transactions on Industrial Electronics*, vol. 40, pp. 521-528, Oct 1993.
[7] F. H. Dupont, V. F. Montagner, J. R. Pinheiro, H. Pinheiro, S. V. G. Oliveira, and A. Péres, "Multiple controllers for boost converters under large load range: a GA and fuzzy logic based approach," Proceedings of the International Conference on Industrial Technologies, Viña del Mar, Chile, 2010.
[8] F. Botteron, H. Pinheiro, H. A. Grundling, J. R. Pinheiro, and H. L. Hey, "Digital voltage and current controllers for three-phase PWM inverter for UPS applications," Proceedings of the Thirty-Sixth IAS Annual Meeting. IEEE Industry Applications Conference Chicago, USA, 2001.
[9] V. F. Montagner, E. G. Carati, and H. A. Grundling, "Design and analysis of a linear quadratic regulator with repetitive controller for AC power supplies " Proceedings of the IEEE International Symposium on Industrial Electronics, Rio de Janeiro, 2003.
[10] S. P. Boyd, L. E. Ghaoui, E. Feron, and V. Balakrishnan, *Linear matrix inequalities in system and control theory*. Philadelphia: Society for Industrial and Applied Mathematics, 1994.
[11] S. Buso and P. Mattavelli, *Digital control in power electronics*: Morgan & Claypool Publishers, 2006.
[12] H. K. Khalil, *Nonlinear systems*, 3 ed. Upper Saddle River, USA: Prentice Hall, 2002.
[13] A. Kugi and K. Schlacher, "Nonlinear H-infinity-controller design for a DC-to-DC power converter," *IEEE Transactions on Control Systems Technology*, vol. 7, pp. 230-237, Mar 1999.
[14] K. Tanaka and H. O. Wang, *Fuzzy Control Systems Design and Analysis: a linear matrix inequality approach*. New York, USA: John Wiley and Sons., 2001.
[15] J. Ackermann, *Robust control : systems with uncertain parameters*. London: Springer-Verlag, 1993.
[16] J. Leyva-Ramos and J. A. Morales-Saldana, "Uncertainty models for switch-mode DC-DC converters," *IEEE Transactions on Circuits and Systems I-Fundamental Theory and Applications*, vol. 47, pp. 200-203, Feb 2000.
[17] I. J. Gabe, V. F. Montagner, and H. Pinheiro, "Design and Implementation of a Robust Current Controller for VSI Connected to the Grid Through an LCL Filter " *IEEE Transactions on Power Electronics*, vol. 24, pp. 1444 - 1452 2009.
[18] C. Olalla, R. Leyva, A. El Aroudi, P. Garces, and I. Queinnec, "LMI robust control design for boost PWM converters," *IET Power Electronics*, vol. 3, pp. 75-85, Jan 2010.
[19] V. F. Montagner and L. D. Peres, "H Infinity Control with Pole Location for a DC - DC Converter with a Switched Load," Proceedings of the IEEE International Symposium on Industrial Electronics 2003.
[20] K. Y. Lian, J. J. Liou, and C. Y. Huang, "LMI-based integral fuzzy control of DC-DC converters," *IEEE Transactions on Fuzzy Systems*, vol. 14, pp. 71-80, Feb 2006.
[21] P. Gahinet, A. Nemirovski, A. J. Laub, and M. Chilali, *LMI Control Toolbox User's Guide*. Natick, USA: The Mathworks Inc., 1995.
[22] J. C. Geromel, P. L. D. Peres, and S. R. Souza, "H_2 guaranteed cost control for uncertain continuous-time linear systems," *Systems & Control Letters*, vol. 19, pp. 23-27, July 1992.
[23] J. Alvarez-Ramirez, G. Espinosa-Perez, and D. Noriega-Pineda, "Current-mode control of DC-DC power converters: a backstepping approach," *Proceedings of the 2001 IEEE International Conference on Control Applications*, 2001, pp. 190-195.
[24] R. D. Middlebrook, "Topics in Multiple-Loop Regulators and Current-Mode Programming," *IEEE Transactions on Power Electronics*, vol. PE-2, pp. 109-124, 1987.

BIOGRAPHIES

Vinícius Foletto Montagner received the B.S. and M.S. degrees in Electrical Engineering from Federal University of Santa Maria in 1996 and 2000, respectively. He received the PhD and post-doctoral degrees in Electrical Engineering from University of Campinas in 2005 and 2006, respectively. Currently, he is a professor at Electric Power Processing Department in Federal University of Santa Maria. His research interests include control theory and applications.

Luiz Antonio Maccari Jr. received the B.S. degree in Electrical Engineering from Federal University of Santa Maria in 2009. Currently, he is master's student in PPGEE from Federal University of Santa Maria. His research interests include robust control and applications.

Humberto Pinheiro received the B.S. degree Electrical Engineering from Federal University of Santa Maria in 1983, the M.S. degree in Electrical Engineering from Federal University of Santa Catarina in 1987, and the PhD in Electrical Engineering from Concordia University, Canada, in 1999. Currently, he is associate professor at Electric Power Processing Department in Federal University of Santa Maria. His research interests include wind power systems and uninterruptible power supply systems.

Ricardo C. L. F. Oliveira received the B.S. degree in Computer Engineering from Pontifical Catholic University of Paraná in 2001. He received M. Sc., the PhD and the post-doctoral degrees in Electrical Engineering from University of Campinas in 2003, and 2006 and 2009, respectively. Currently, he is a professor at Department of Telematics, School of Electrical and Computer Engineering, University of Campinas. His research interests include linear systems and control theory.